Scilight

Innovations in Water Treatment

https://www.sciltp.com/journals/iwt

Review

Spent Battery-Derived Materials for Wastewater Treatment

Zhiqian Xu [1], Zhijie Chen [1,*], Zhiliang Wu [2], Xiang-Yang Lou [3], Xuran Liu [1], Bing-Jie Ni [1,*]

[1] UNSW Water Research Centre, School of Civil and Environmental Engineering, University of New South Wales, Sydney, NSW 2052, Australia
[2] Discipline of Chemical Engineering, Western Australian School of Mines: Minerals, Energy and Chemical Engineering, Curtin University, GPO Box U1987, Perth, WA, 6845, Australia
[3] Institute of Technology for Future Industry (School of Science and Technology Instrument Application Engineering), Shenzhen Institute of Information Technology, Shenzhen 518172, China
* Correspondence: zhijie.chen1@unsw.edu.au (Z.C.); bingjieni@gmail.com (B.-J.N.)

How To Cite: Xu, Z.; Chen, Z.; Wu, Z.; et al. Spent Battery-Derived Materials for Wastewater Treatment. *Innovations in Water Treatment* **2025**, *1*(1), 2.

Received: 15 July 2025
Revised: 3 September 2025
Accepted: 4 September 2025
Published: 8 September 2025

Abstract: The rapid growth of energy storage technologies has led to a surge in spent battery waste, presenting both environmental challenges and opportunities for resource recovery. Emerging research highlights the potential of repurposing battery-derived components into functional materials for wastewater remediation. This review presents a comprehensive overview of recent advances in synthesizing catalysts and adsorbents from spent batteries, with a particular focus on their application in advanced oxidation processes (AOPs) and pollutant adsorption. Key synthesis methods, catalytic mechanisms, and the roles of material properties—such as surface area, defect structures, and heteroatom doping—are critically examined. By bridging materials science and environmental engineering, this work underscores the potential of battery waste valorization and provides guidance for scaling these technologies toward real-world wastewater treatment applications.

Keywords: waste utilization; wastewater treatment; catalysts; composites; pollutant adsorption

1. Introduction

The widespread use of portable electronic devices, electric vehicles, and renewable energy storage systems has led to an exponential growth in global battery consumption [1–5]. Consequently, the disposal of spent batteries, containing toxic heavy metals, electrolyte residues, and complex material compositions, has posed serious challenges to both environmental safety and resource recovery [6–9]. However, these spent batteries contain valuable transition metals (e.g., cobalt, manganese, nickel, zinc) and carbon-based components, offering unique opportunities for resource valorization [10–18]. Recently, developing effective strategies to convert spent batteries into functional materials has attracted increasing attention. Under this context, various components of spent batteries, such as transition metals and carbon-based electrodes, have been converted into functional materials through methods such as hydrothermal synthesis, sol-gel processes, and co-precipitation [19].

Until now, various types of materials of spent batteries, including lithium-ion batteries (LIBs) (Figure 1a) [20], such as lithium iron phosphate ($LiFePO_4$), lithium cobalt oxide ($LiCoO_2$) [21,22], lithium manganese oxide ($LiMn_2O_4$), as well as other battery types such as alkaline zinc–manganese (Zn–Mn) batteries (Figure 1b), and carbon–zinc dry cells (Figure 1c), have been successfully converted into functional materials (such as catalysts and adsorbents) [23–35] for wastewater treatment applications. Although several review papers have addressed the synthesis of catalysts and adsorbents from various waste sources (such as biomass, industrial residues, and electronic waste) for applications in adsorption, AOPs, photocatalytic degradation, and electrochemical treatments [36–41], a comprehensive review specifically focusing on spent battery-derived functional materials for wastewater

purification remains lacking. This gap limits our understanding of their full potential in wastewater remediation and the strategic upcycling of electronic waste.

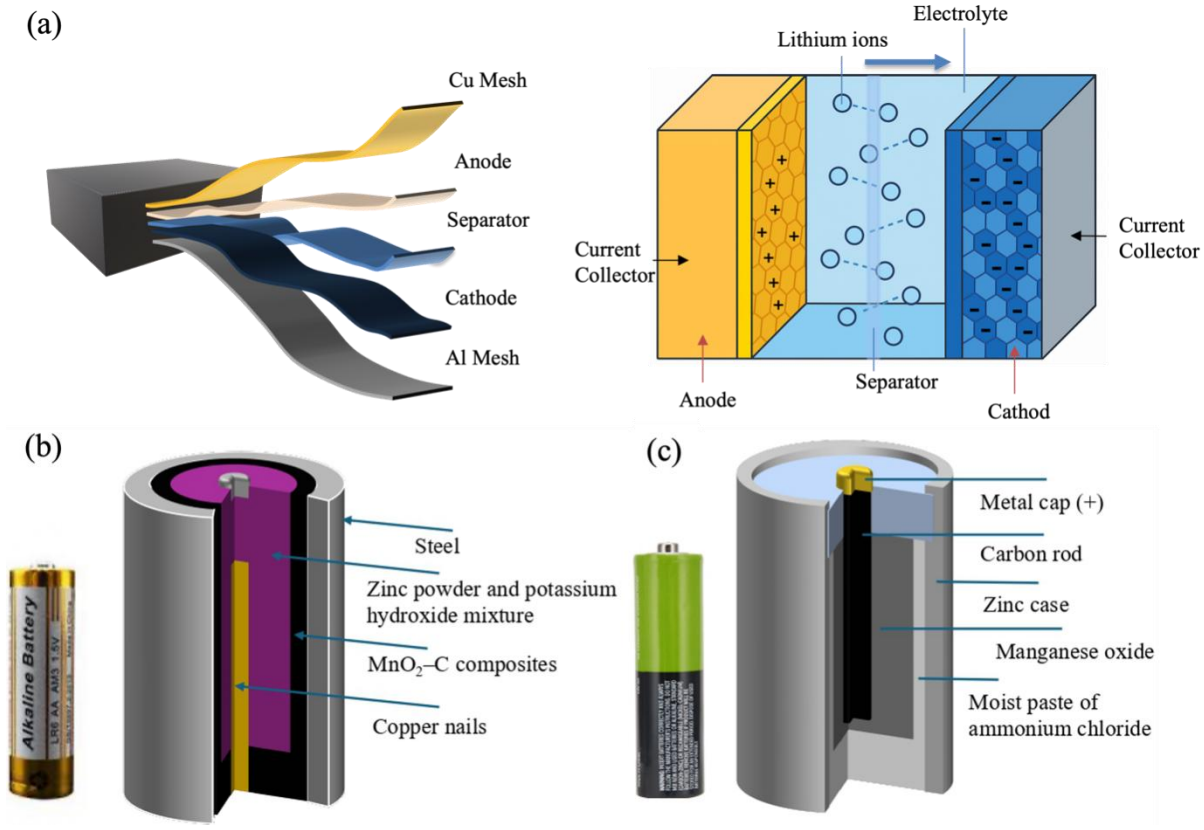

Figure 1. (**a**) The standard components and operation of LIBs. (**b**) The standard components of alkaline Zn–Mn batteries. (**c**) The standard components of carbon–zinc dry cells.

This review aims to provide a comprehensive overview of recent advancements in wastewater remediation using functional materials derived from spent batteries. First, we present key pretreatment methods for processing spent batteries, followed by a summary of effective strategies to convert battery waste into high-value functional materials, along with a discussion of relevant experimental parameters. Subsequently, we examine the application of these materials in AOPs and adsorption, with particular emphasis on designing high-performance catalysts through the modulation of intrinsic and extrinsic material properties. Finally, this review outlines future perspectives on the development of next-generation battery waste-derived materials for sustainable wastewater treatment.

2. Methods for Converting Spent Batteries to Functional Materials

2.1. Pretreatment for Spent Batteries

Pretreatment, the initial step in recovering waste LIBs, plays a vital role before further converting spent batteries into useful materials. Some effective pretreatments can improve recovery efficiency and reduce the energy consumption of the follow-up steps [42–44]. Based on previous research, pretreatments mainly include four important steps: discharging, dismantling, crushing, and separation [45,46]. Figure 2 illustrates the performance comparison of the four pretreatment steps across multiple dimensions in terms of cost level, recovery efficiency, process complexity, environmental impact, and safety risk.

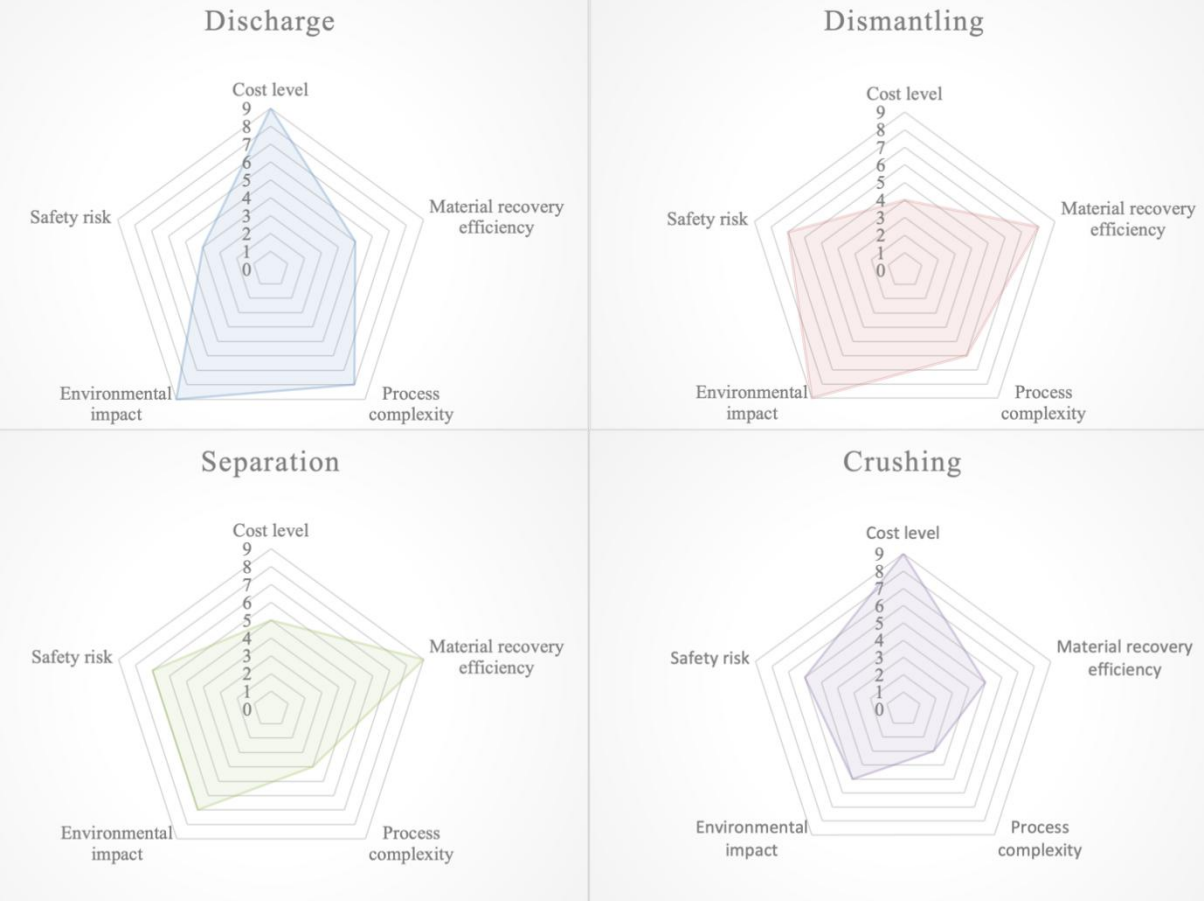

Figure 2. The performance comparison of the four pre-treatment steps across multiple dimensions [45,47–49]. (The maximum score is 9, with higher scores indicating better performance in each respective aspect.)

2.1.1. Discharge

Due to the residual electrolyte and electricity in spent LIBs, discharging is a necessary pretreatment step to prevent fire or explosion risks caused by short circuits or sparks [50–52]. Chemical discharge is the most widely used due to its high efficiency and operational safety by immersing LIBs in salt solutions. However, common salt solutions like NaCl can cause severe corrosion, leading to electrolyte leakage, reduced metal recovery, and high wastewater treatment costs [53]. Furthermore, voltage rebound may occur after 48 h, compromising safety and measurement accuracy [54,55]. Using flake graphite to suppress voltage recovery offers a safer and cleaner solution [56].

2.1.2. Dismantling and Crushing

After the residual electricity in LIBs is safely discharged, further treatment such as opening the battery shell can be performed more safely. Common methods include dismantling and crushing [57]. Dismantling usually involves separating the modules and cells, removing the casing, detaching wires, cleaning off adhesives, and removing binders. Most dismantling is still done manually because the wide variety of battery types and degraded components, such as screws, make automation difficult [58–61]. Crushing is another widely used method. Crushing can be done through dry or wet crushing. To reduce risks, dry crushing is often performed in an inert gas environment such as nitrogen, argon, or carbon dioxide to prevent fires or toxic gas release [62–64]. Although crushing is more efficient, it usually results in lower material purity [65,66].

2.1.3. Separation

After dismantling and crushing LIBs, additional separation steps are needed to recover valuable materials such as plastics, metal casings, copper or aluminium foil, separators, and binders. Common physical separation methods include sieving, electrostatic separation, gravity separation, flotation, and eddy current separation [57,67–72]. Sieving uses particle size differences, while electrostatic and gravity methods exploit electrical conductivity and density contrasts, respectively [73–76]. Flotation separates materials based on surface hydrophilicity, with hydrophobic

particles attaching to bubbles and being collected [77,78]. Eddy current separation uses magnetic fields to induce motion in conductive metals, allowing them to be sorted by trajectory [79–82]. Chemical methods focus on removing metal foils or binders. For example, strong alkaline solutions can dissolve aluminium foil efficiently but generate waste liquid [83]. A newer method uses water electrolysis to generate gases that help detach electrode materials from collectors, offering a cleaner recovery option [84].

2.2. Methodologies for High-Value Materials Synthesis

2.2.1. Hydrothermal Synthesis

Hydrothermal synthesis is a chemical technique that utilizes elevated temperature and pressure within a sealed environment to facilitate the formation of functional materials. The typical process begins with acid leaching [85–88] or green bioleaching solution [89], enabling the release of valuable metal ions and active components from spent lithium-ion batteries. The extracted species are then subjected to hydrothermal treatment under controlled conditions. For instance, the synthesis of MnO_2 and MnO_2-loaded nano-zero-valent iron composites begins by mixing $LiMn_2O_4$ with an H_2SO_4 solution, followed by hydrothermal treatment at 140 °C for 24 h [90]. Moreover, graphene oxide (GO) is commonly synthesized via a modified Hummers' method, using waste graphite or dry cell carbon rods recovered from spent battery anodes as carbon precursors [91–93], typically followed by hydrothermal heating (e.g., 180 °C for 24 h) in a Teflon-lined reactor. Subsequently, the synthesized products undergo standard post-treatment procedures such as washing with deionized water or ethanol, centrifugation, and drying, ultimately yielding the final functional materials with desired purity and structure. In addition to spent lithium-ion batteries, carbon powder recovered from spent dry batteries can also benefit from this synthesis methodology, enabling its transformation into functional materials with tailored surface properties and structure [94].

2.2.2. Sol-Gel Synthesis

The sol–gel method has been widely employed for synthesizing functional materials from spent batteries. This technique offers a sustainable and effective approach for transforming valuable elements into advanced materials for water purification. Compared to conventional chemical synthesis methods, the sol–gel process allows precise control over composition, surface properties, and morphology under relatively mild conditions. For sol-gel method, metal ions such as Fe^{3+}, Mn^{2+}, and Zn^{2+} are first recovered from the anode and cathode materials of spent batteries via acid leaching or alkaline dissolution, forming metal-rich precursor solutions [29,30,95,96]. These solutions are then directly utilized in sol–gel synthesis. Chelating agents such as citric acid or ethylene glycol are typically added to stabilize the metal species and prevent premature precipitation. Controlled hydrolysis and condensation reactions are subsequently initiated through pH adjustment, leading to the formation of a stable gel network. The generated gel is first dried and subsequently calcined at moderate temperatures (typically 400–600 °C), yielding metal oxide materials with high surface area and abundant reactive sites. Recently, several studies have demonstrated the successful synthesis of $ZnFe_2O_4$/g-C_3N_4 photocatalysts [30], $LaCoO_3$/Co_3O_4 nanocomposites [97], and $Mn_{0.27}FeO_{4.55}$ bimetallic oxides [98] via the sol–gel method using materials recovered from spent batteries for wastewater treatment applications. These materials exhibit excellent performance in the removal of heavy metals, dyes, and even pharmaceutical contaminants. Moreover, carbonaceous components such as graphite or carbon black can also be incorporated into the sol–gel matrix, resulting in materials with significantly enhanced surface area and catalytic performance [99].

2.2.3. Co-Precipitation

Co-precipitation is a widely used wet chemical method for synthesizing metal-based functional materials [100]. Co-precipitation typically involves the simultaneous precipitation of two or more metal ions from a homogeneous solution, achieved by adjusting the pH using precipitants such as NaOH, NH_4OH, or Na_2CO_3. In the context of spent battery recovery, valuable metal ions such as Fe^{3+}, Mn^{2+}, Co^{2+}, Ni^{2+}, and Zn^{2+} are first extracted from the leaching of anode and cathode materials through acid or alternative leaching methods [101–104]. The resulting metal ion-containing solution then serves as the precursor for co-precipitation. Precipitants are gradually added to the solution to promote uniform nucleation and minimize particle aggregation. Factors such as temperature, pH, ion concentration, and stirring speed significantly influence the morphology, crystallinity, and surface properties of the final material. The resulting precipitates—typically metal hydroxides or carbonates—are purified by filtration, centrifugation, and successive washing steps. These intermediates are then converted into oxides or mixed metal oxides by drying and calcination at temperatures typically ranging from 300 to 600 °C. Compared to other synthesis techniques, co-precipitation is cost-effective, scalable, and environmentally friendly. These

advantages make it particularly suitable for producing functional materials derived from battery waste, which can be further applied in environmental remediation, including adsorption, catalysis, and advanced oxidation processes.

2.2.4. Calcination

Calcination is a widely used thermal treatment technique for synthesizing functional materials from spent batteries, particularly for applications in wastewater treatment. This process involves heating precursor materials to elevated temperatures, typically between 300 °C and 800 °C, under a specific atmospheric condition, usually air or oxygen. Calcination induces thermal decomposition, phase transitions, and crystallization, while simultaneously removing volatile components such as water, carbonates, nitrates, and organic binders. In battery recycling, calcination can be employed either as a standalone method or as a final step following other synthesis routes such as co-precipitation, sol-gel, or hydrothermal techniques [105,106]. After discharging, leaching (acidic or alkaline), and mechanical separation, precursor compounds containing valuable elements like Al, Zn, Fe, Ni, Co, or graphite can be extracted. These precursors are then subjected to calcination to yield high-purity metal oxides, such as $ZnFe_2O_4$, CuO, and $CuFe_2O_4$, or efficient carbon-based catalysts with enhanced surface area, structural stability, and catalytic activity [95,105,107,108]. These calcined oxides and carbon-supported materials are highly effective in wastewater treatment due to their strong redox properties, high adsorption capacities, and stability in both acidic and alkaline environments. For example, zinc ferrite ($ZnFe_2O_4$) has been successfully applied for the removal of bisphenol A (BPA) [95], while a thermally treated graphite catalyst has demonstrated excellent performance in degrading atrazine (ATZ) [109]. Furthermore, calcination parameters, including temperature, duration, and heating rate, play a crucial role in determining the final material's particle size, surface structure, porosity, and crystallinity, all of which directly impact their efficiency in pollutant removal applications [110].

2.2.5. Flash Joule Heating and Other Methodologies

Flash Joule heating (FJH) is an advanced technique for upgrading iron-rich residues obtained after extensive lithium extraction from $LiFePO_4$ batteries. In the FJH process, an electric current is directly applied to the sample, rapidly generating extremely high temperatures [111,112]. The electricity also induces both stripping and quenching effects. The intense heat and electric field break Fe–O bonds, resulting in the formation of zero-valent iron species, which exhibit strong catalytic activity [113]. Recently, materials synthesized via the FJH method have been successfully applied in the degradation of antibiotic contaminants, such as chloramphenicol (CAP), during wastewater treatment [114].

Some researchers have investigated the utilization of waste LIB materials to synthesize catalysts through alternative methods. Ball milling is a widely used mechanical synthesis method and operates through repeated impact and shear forces generated by high-speed rotation without high temperature [115–118]. The ball milling enables the physical crushing and average mixing of materials, while also promoting subsequent chemical reactions, making it highly effective for preparing nanostructured and composite materials. However, the ball milling also might produce uneven distribution of product size and introduce some impurities into the product [119,120]), For example, Waste graphite from LIBs can be mixed with $KMnO_4$ and stainless steel balls in a high-energy ball mill to produce functional materials capable of adsorbing heavy metals such as Cu^{2+}, Pb^{2+}, and Cd^{2+} [121].

Ultrasonic exfoliation is a simple and highly effective physical method commonly used to strip bulk graphite, graphite oxide, and other layered materials into graphene or GO [122–124]. The ultrasonic exfoliation relies on cavitation effects in liquids, which generate localized high temperatures and pressures that break the van der Waals forces between layers, enabling physical exfoliation [125]. The ultrasonic exfoliation is easy to operate, environmentally friendly, and does not introduce additional chemicals or contaminants. However, ultrasonic exfoliation is energy-intensive, has relatively low yield, and is highly sensitive to factors [126,127] such as ultrasonic duration, power, solvent type, and processing conditions. Notably, it is often combined with other synthesis techniques [128], such as the Hummers [129] and ball milling methods [130], to produce high-performance functional materials. For example, after hummers method treatment, the waste graphite can be oxidized into graphite oxide and subsequently exfoliated ultrasonically to form GO, which also exhibits high adsorption capacity for heavy metals [131].

Besides these synthetic methods (Table 1), the direct use of untreated LIB powders was also investigated. For example, two common wastewater pollutants, ammonia nitrogen (NH_4^+-N) and halogenated phenolic compounds such as 2,4,6-trichlorophenol, have been effectively removed using LIB powders derived from spent LIB materials [132]. Moreover, zinc-catalyzed glycolysis, though primarily used for PET depolymerization, has shown potential in dye removal. The reduction capacity of zero-valent zinc (Zn^0) plays a key role in converting colored PET bottles into colorless products, indicating its possible application in the degradation or decolorization of dye pollutants [133].

Table 1. The comparison of different synthesis methodologies for waste battery-derived materials.

Method	Precursors	Temperature	Advantages	Limitations	Ref.
Hydrothermal synthesis	Leachate (metal ions), waste graphite	140–180 °C	Mild conditions, low emissions	Time-consuming, autoclave demand	[89,94]
Sol-gel synthesis	Metal ion solutions, chelating agents	400–600 °C (post-calcination)	Good control of morphology and surface, eco-friendly, low toxic byproducts	Sensitive to pH and gelation	[97,98]
Co-precipitation	Mixed metal ion solutions	300–600 °C (post-calcination)	Low cost, low hazard, scalable	Limited particle size control	[100,134,135]
Calcination	Dried precursors (e.g., hydroxides, carbonates)	300–800 °C	Simple, enhances crystallinity and activity	High energy consumption, CO_2 emissions	[95,109]
Flash Joule heating	Iron-rich residues	>1000 °C (instant)	Ultra-fast, minimal waste	Equipment demanding, high energy burst	[113,114]
Ball milling	Waste graphite, oxidants/precursors	Room temperature	Low cost, no solvent	Particle size irregularity, mechanical wear, potential metal debris	[119–121]
Ultrasonic exfoliation	Graphite or layered materials	Room temperature	No chemicals needed, eco-friendly	Low yield, high energy input	[125–127]

3. Applications of Spent Battery-Derived Materials for Wastewater Treatment

3.1. AOPs for Contaminant Removal

With the rapid accumulation of spent lithium-ion, alkaline, and other types of batteries, increasing attention has been paid to the reutilization of their recovered materials as catalysts in AOPs for wastewater treatment [37,136,137]. These waste-derived catalysts, either directly reused or synthesized via physicochemical modifications, can effectively activate common oxidants such as hydrogen peroxide (H_2O_2), peroxymonosulfate (PMS), or peroxydisulfate (PDS). Upon activation, these oxidants produce a series of highly reactive oxygen species (ROS), including hydroxyl radicals (·OH), sulfate radicals ($SO_4^{\cdot-}$), and singlet oxygen ($^1O_2$). These species play a critical role in degrading a wide range of organic pollutants, including dyes, pharmaceuticals, halogenated compounds, and endocrine-disrupting chemicals.

3.1.1. Sulfate Radical-Induced AOPs for Pollutant Removal

Sulfate radical-based advanced oxidation processes (SR-AOPs) have attracted increasing attention owing to the favorable characteristics of $SO_4^{\cdot-}$ [138], including their relatively long half-life (30–40 μs), high redox potential (2.5–3.1 V vs. normal hydrogen electrode (NHE)), and rapid reaction kinetics with organic pollutants (rate constants ranging from 10^6 to 10^9 $M^{-1}\cdot s^{-1}$) [139]. Highly reactive $SO_4^{\cdot-}$ can be effectively generated through the activation of PMS or PDS by various approaches, including ultrasonic, ultraviolet (UV) light, thermal treatment, catalytic activation [140,141]. Currently, a critical challenge lies in the development of cost-effective catalysts for the activation of PDS/PMS, and spent battery-derived materials have demonstrated great potential owing to their low cost, high catalytic activity, and environmental sustainability [137]. The characteristics of representative spent battery-derived materials are concluded in Table 2.

The SR-AOPs materials can be categorized into several types. Catalytic activation by transition metals is the most widely applied approach. For instance, β-MnO_2 derived from waste LIB cathode materials was found to effectively activate PMS, achieving 95.2% degradation of sulfadiazine (SDZ), primarily through $SO_4^{\cdot-}$-mediated oxidation [85]. Another example is CM-850, a Co-rich material derived from the cathode of spent LIBs, utilizes the redox cycling of Co^{2+}/Co^{3+} to activate PMS and achieve 94% removal of levofloxacin (LFX) within 60 min. Notably, it also maintains high catalytic stability over four consecutive cycles [106]. Ternary metal oxide catalysts, such as CM-650 (Ni/Co/Mn oxides), have demonstrated excellent performance in degrading iopamidol (IPM). The enhanced activity is attributed to the synergistic interactions among multiple redox-active metal ions and efficient PMS activation through redox pair transitions, including Co(III)/Co(II), Mn(IV)/Mn(III), Mn(III)/Mn(II), and Ni(III)/Ni(II) [107].

Carbon materials derived from spent battery anodes have also shown excellent performance in PMS activation. For example, TG-800, a carbon catalyst obtained by calcining waste graphite at 800 °C, shows rapid degradation of ATZ, achieving 99.2% removal within six minutes. In the TG-800/PMS system, multiple reactive

species, including $SO_4^{\cdot-}$, ·OH, $^1O_2$, and direct electron transfer, participate in the degradation process. The C=O functional groups on the carbon surface were identified as the main active sites responsible for PMS activation [142]. These findings demonstrate the potential to transform low-value spent graphite into high-performance environmental catalysts. In the case of photocatalysis, $ZnFe_2O_4$/g-C_3N_4 (ZFO-CN), an S-type heterojunction material prepared from zinc–manganese batteries, achieves over 97.7% removal of BPA under visible light and PMS activation [30]. The ZFO-CN/PMS system generates a variety of reactive species, including $^1O_2$, photogenerated holes (h^+), $SO_4^{\cdot-}$, and ·OH, showing strong potential for solar-assisted wastewater treatment. Even the combination of pure $ZnFe_2O_4$ and PDS under light exhibited high degradation performance [95]. Similarly, zinc–manganese bimetallic oxide (ZMBO), synthesized from spent alkaline zinc–manganese batteries, activates PMS efficiently and removes 90.0% of BPA within 120 min [143]. The Mn component contributes to PMS activation through redox cycling, while the Zn component enhances visible-light responsiveness, further improving catalytic performance. Lastly, synergistic and mixed activation mechanisms have emerged as promising strategies. Such results highlight the broader potential of PMS-based systems to go beyond single-contaminant degradation and target complex pollutant mixtures through cooperative pathways.

Table 2. Summary of representative spent battery-derived catalysts for SR-AOPs.

Catalyst	Source	Target Pollutant	Oxidant	Removal Efficiency	Ref.
β-MnO_2	Spent LIB cathode	SDZ	1 mM PMS	95.2% in 2 h	[85]
CM-850	Spent LIB cathode	LFX	0.5 mM PMS	94% in 60 min	[106]
CM-650	Spent LIBs	IPM	0.2 mM PMS	100% in 20 min	[107]
TG-800	Spent battery anode graphite	ATZ	0.2 mM PMS	99.2% in 6 min	[142]
ZFO-CN	Spent Zn–Mn batteries	BPA	0.5 mM PMS	>97.7% under visible light in 60 min	[30]
ZMBO	Spent alkaline Zn–Mn batteries	BPA	1.00 mM PMS	90.0% in 120 min	[143]

3.1.2. Hydroxide Radical-Induced AOPs for Pollutant Removal

In hydroxyl radical-induced advanced oxidation processes (·OH-AOPs), ·OH serves as the primary reactive species. These radicals are highly potent and non-selective oxidants, with a high standard redox potential of approximately 2.8 V vs. NHE (pH = 0) [144]. Despite their strong oxidative capacity, ·OH radicals possess an extremely short lifetime, typically ranging from 10^{-6} to 10^{-3} s [145], which necessitates their in-situ generation during pollutant degradation. The ·OH can be generated in situ through various methods, including the use of oxidants like H_2O_2, catalytic agents such as Cu^{2+} and carbon-based materials, and irradiation techniques like UV light exposure [146,147]. Once generated, ·OH initiates pollutant degradation through three main pathways [145]. ·OH can degrade organic pollutants through several mechanisms. One involves the abstraction of hydrogen atoms, which generates highly reactive radical intermediates. Another pathway is the addition of ·OH to aromatic rings or carbon–carbon double bonds, which destabilizes the molecular structure of contaminants. A third route relies on electron transfer processes that lead to the breakdown of complex organic compounds. Together, these mechanisms enable ·OH to act as a rapid and non-selective oxidant for a broad spectrum of environmental pollutants. Representative spent battery-derived catalysts for ·OH-AOPs characteristics are concluded in Table 3.

Table 3. Summary of representative spent battery-derived catalysts for ·OH-AOPs.

Catalyst	Source	Target Pollutant	Oxidant	Removal Efficiency	Ref.
$CuFe_2O_4$	Spent LIBs	MB	0.3 M H_2O_2	96.1% MB degradation in 45 min	[101]
$CoFe_2O_4$	Spent LIBs	MB	3% (*v*/*v*) H_2O_2 8.0 mL	87.7% MB degradation in 45 min	[102]
FPOH	Spent $LiFePO_4$ batteries	Pb^{2+}, MB	5 mL H_2O_2	Pb^{2+}: 43.203 mg/g, 100% MB degradation in 12 h	[88]
MnO_2/Fe^0	Spent LIBs	SDZ	6 mM H_2O_2	98.6% SDZ degradation in 60 min	[90]
SULM	Spent $LiFePO_4$ batteries	RhB	4 mM H_2O_2	99.8% RhB degradation in 30 min	[87]
ZVI/EG	Spent LIBs	4-CP	2.2 mM H_2O_2	97% 4-CP removal in 60 min	[148]
Modified graphite from LIBs residues	Spent LIBs	Oxalic acid	Ozone flow rate: 100 mL/min, ozone concentration: 30 mg/L	95% oxalic acid degradation in 1 h	[149]
CDs	Spent dry batteries	BTB	2 mL H_2O_2	84% BTB removal in 180 min	[94]

Iron-based Fenton catalysts can be synthesized using spent lithium-ion batteries. For instance, cobalt and copper recovered from these batteries have been used to prepare cobalt ferrite ($CoFe_2O_4$) and copper ferrite ($CuFe_2O_4$) catalysts, exhibiting high MB degradation efficiencies (87.7% and 96.1% respectively) under photo-Fenton conditions, with low metal leaching and good reusability [101,102]. Similarly, the ferric phosphate hydroxy complex (FPOH), extracted from the cathode material of spent $LiFePO_4$ batteries, exhibits effective performance in both heavy metal adsorption and organic dye degradation [88]. It achieves a maximum Pb^{2+} adsorption capacity of 43.203 mg/g and can degrade methylene blue (MB) within 12 h completely. A MnO_2/Fe^0 composite synthesized from recovered manganese achieves approximately 98.6% degradation of SDZ. This high efficiency is attributed to the presence of nano zero-valent iron , which provides abundant active sites and shows a synergistic effect with MnO_2 and light irradiation [90]. A sea urchin-like $LiFePO_4$-derived material (SULM), combined with hydroxylamine and H_2O_2, significantly enhances the generation of ·OH and $^1O_2$, leading to effective organic pollutant removal [87]. Zero-valent iron supported on graphite (ZVI/EG) also demonstrates strong catalytic activity toward 4-chlorophenol (4-CP) removal (up to 97%) by facilitating redox cycling of interfacial Fe(III)/Fe(II) and solution-phase Fe species, with sustained performance over multiple cycles [148]. Additionally, a Bi_2WO_6/boron-doped reduced graphene oxide (BWO/BR) nanocomposite, formed by integrating spent LIB-derived boron-doped reduced graphene oxide (BRGO) with Bi_2WO_6 (BWO), exhibits a narrower band gap (reduced from 2.73 eV to 2.22 eV), which enhances light absorption and charge separation efficiency. Under visible light and natural sunlight, the BWO/BR system achieves high degradation efficiencies for antibiotics such as tetracycline hydrochloride (TCH, 93%) and ciprofloxacin (CIP, 97.5%). The degradation mechanism primarily involves the generation of ROS, including ·OH, superoxide radicals ($\cdot O_2^-$), and h^+, with a synergistic effect among them. Moreover, BWO/BR significantly reduces the antimicrobial activity of the treated water, mitigating potential environmental toxicity risks [93]. In addition, modified graphite (A350-2) derived from LIBs acid-leaching residues effectively catalyzes the ozonation of oxalic acid about 95% within 1 h, where pyridinic nitrogen and surface defects were identified as key active sites for ·OH generation (Figure 3) [149]. From spent dry batteries, $ZnMn_2O_4$ nanoparticles degraded 92% of MB under visible light, primarily through $\cdot O_2^-$ and h^+ pathways [150]. Furthermore, carbon dots (CDs) synthesized from battery waste achieved 84% degradation of bromothymol blue (BTB) dye under sunlight in the presence of H_2O_2, while also exhibiting selective heavy metal detection capability [151].

3.1.3. Singlet Oxygen-Induced AOPs for Pollutant Removal

$^1O_2$, a non-radical reactive oxygen species, typically exhibits a relatively longer lifetime of around 2–4 μs, a lower redox potential (0.81 V vs. NHE), and a higher concentration in water (10^{-14}–10^{-11} mol/L) compared to ·OH or $SO_4^{\cdot-}$ [152,153]. Unlike ·OH and $SO_4^{\cdot-}$ highly reactive free radicals, $^1O_2$ reacts selectively with electron-rich functional groups such as amines, phenols, and sulfur-containing compounds. Owing to this selective reactivity, $^1O_2$ plays a critical role in the targeted degradation of specific organic pollutants, making it valuable for AOPs in complex environmental matrices [154]. Table 4 summarizes the characteristics of spent battery-derived catalysts for $^1O_2$-AOPs.

Transition metal oxides derived from battery cathodes can activate PMS through both radical and non-radical pathways, with $^1O_2$ often serving as the dominant reactive species. For example, $MnCO_3$ synthesized from spent zinc–manganese batteries demonstrates outstanding degradation performance for oxytetracycline hydrochloride (OTC-HCl), achieving 91.3% removal efficiency and 63.6% TOC reduction within just 10 min [155]. Quenching tests and electron paramagnetic resonance (EPR) analysis confirmed $^1O_2$ as the principal oxidant. Additionally, NCM-650 ($LiNi_{0.5}Co_{0.2}Mn_{0.3}O_2$), also derived from spent LIB cathode scraps, achieves complete removal of Rhodamine B (RhB) within 25 min via PMS activation [156]. In the NCM-650/PMS system, although various reactive species (e.g., $SO4^{\cdot-}$, ·OH, $\cdot O_2^-$) play auxiliary roles, density functional theory (DFT) calculations and HPLC-MS analysis highlight the dominance of the non-radical $^1O_2$ pathway in the degradation mechanism. By recovering cobalt from spent LIBs using EDTA-2Na and $NaNO_3$, a Co–NC metal–carbon composite was synthesized with an ultrahigh specific surface area (>3700 m^2/g) [157]. In the Co–NC/PMS system, $^1O_2$ was identified as the sole reactive oxygen species, confirmed by quenching experiments and EPR. DFT simulations revealed the formation mechanism of $^1O_2$ through a sequential pathway: PMS → $^*OH$ → $^*O$ → $^1O_2$. Waste graphite was successfully upgraded via ammonia treatment to form defect-rich, nitrogen-doped graphene (SNGO-2) [91]. This material exhibits excellent catalytic activity, achieving 100% degradation of RhB within 10 min across various water matrices. EPR and scavenger assays confirmed $^1O_2$ as the main ROS, and the synergistic effect of nitrogen doping and structural defects enhance the degradation of RhB. N-doped carbon materials, obtained by calcining battery graphite, also demonstrates efficient PMS activation under a broad pH range. In these systems, C=O groups and graphite-N sites were responsible for $^1O_2$ generation and the subsequent removal of RhB. In

another study, a LIB/PMS system simultaneously achieved nearly 100% removal of trichlorophenol (TCP) and oxidation of coexisting ammonium (NH_4^+) [132]. The dechlorination reaction of TCP is mainly driven by $^1O_2$ and the oxidation of NH_4^+ to N_2 was primarily driven by ClO·, illustrating the versatility of $^1O_2$-based processes for handling complex or mixed contaminant systems.

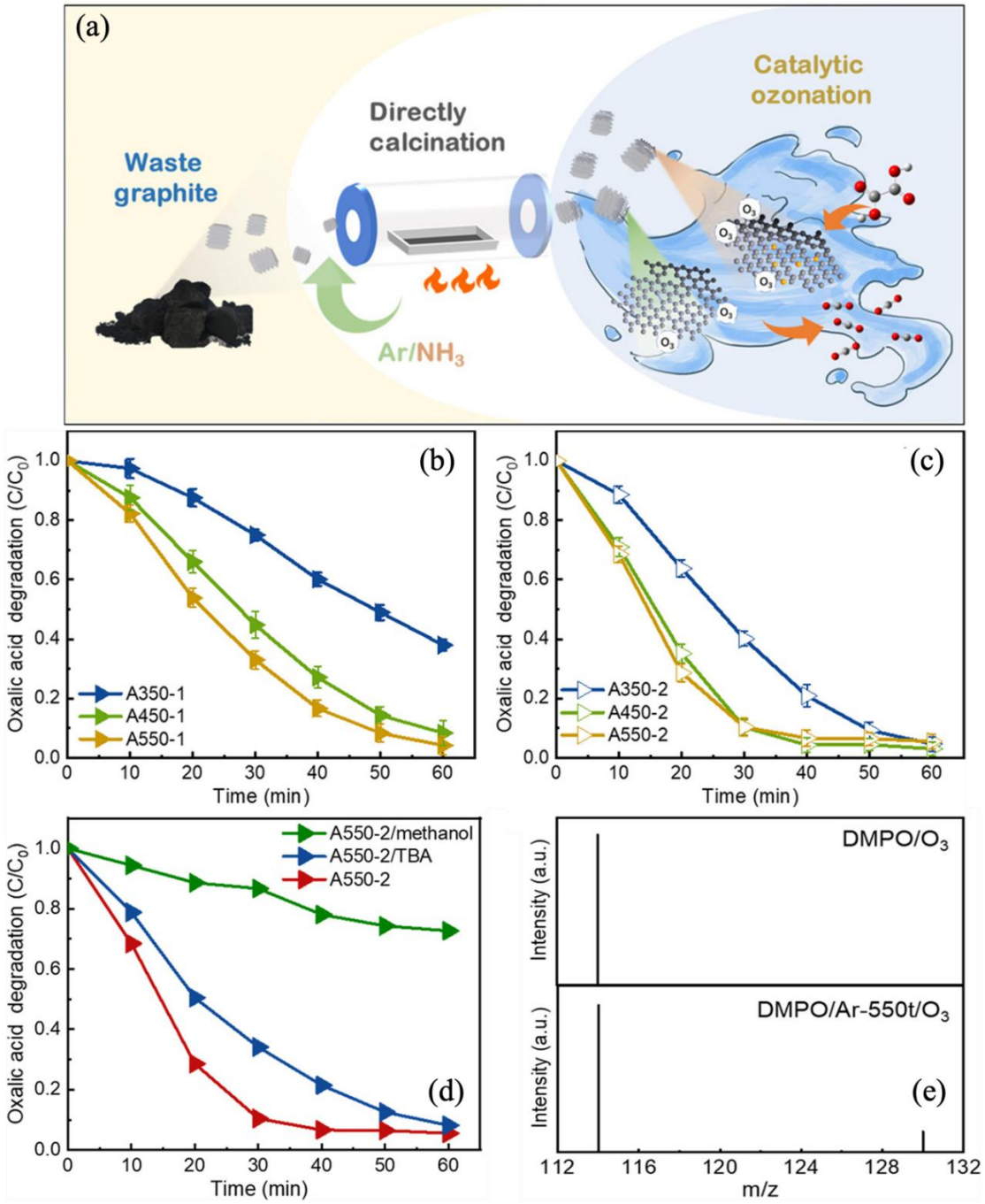

Figure 3. (**a**) Synthesis process of the modified graphite material. (**b**) Oxalic acid removal using the A-1 catalyst and (**c**) the A-2 catalyst. Identification of the dominant reactive oxygen species (·OH) through (**d**) quenching experiments and (**e**) mass spectrometry [149].

Table 4. Summary of representative spent battery-derived catalysts for $^1O_2$-AOPs.

Catalyst	Source	Target Pollutant	Oxidant	Removal Efficiency	Ref.
$MnCO_3$	Alkaline Zn-MnO_2 dry batteries	OTC-HCl	0.4 g/L PMS	91.3% OTC-HCl degradation, 63.6% TOC removal in 10 min	[155]
NCM-650	Spent LIBs	RhB	1 mM PMS	Complete RhB degradation in 25 min	[156]
Co–NC	Spent LIB cathodes	BPA	0.1 g/L PMS	100% BPA degradation in 10 min	[157]
SNGO-2	Spent graphite from spent LIBs	RhB	0.3 g/L PMS	100% RhB degradation in 10 min	[91]
LIB material	Spent LIBs	TCP	4.5 mM PMS	100% TCP degradation rate, 93.7% NH_4^+ -N removal rate in 60 min	[132]

3.2. Pollutant Adsorption

To promote the sustainable recycling of spent batteries, increasing research efforts have been devoted to converting battery waste into high-performance adsorbents for environmental remediation, particularly in the field of wastewater treatment [25,38]. Due to the complexity and diversity of battery components, including anode materials, cathode materials, separators, and electrolytes, various valuable elements can be recovered and utilized to synthesize functional adsorbents [158]. Such materials exhibit unique physical and chemical properties, such as high surface area, abundant functional groups, tunable porosity, and redox activity, enabling effective interactions with a wide range of water pollutants, including heavy metals, dyes, and antibiotics, etc. A summary of the key characteristics of representative spent battery-derived adsorbents is presented in Table 5.

Porous carbon-based materials, such as nitrogen/oxygen-doped graphene aerogels [159] and urea-assisted pyrolytic carbon (Figure 4) [160], are typically developed from waste graphite anodes or polymeric separators. These materials possess a high specific surface area, well-developed porosity, and abundant surface functional groups, which enable strong interactions with pollutants through mechanisms such as π–π stacking, pore filling, hydrogen bonding, and electrostatic attraction. They have demonstrated excellent removal capabilities for heavy metals and organic contaminants, with maximum adsorption capacities of up to 152.70 mg/g for Pb^{2+} and 330.77 mg/g for MB, respectively.

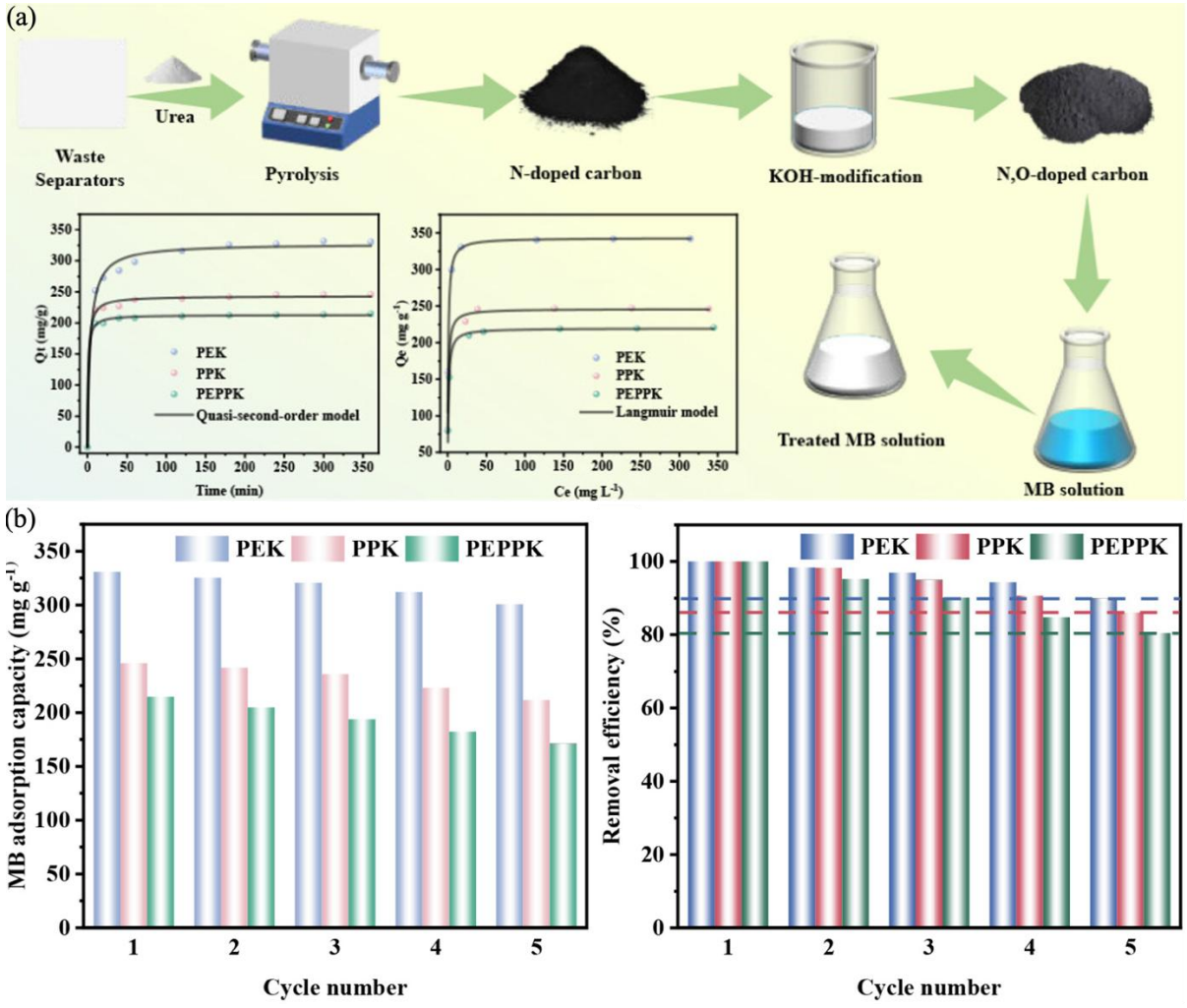

Figure 4. (**a**) The MB adsorption performance of urea-assisted pyrolytic carbon, along with its corresponding adsorption curve. (**b**) MB adsorption capacity and removal efficiency of PEK, PPK, and PEPPK across five consecutive cycles [160].

Table 5. Summary of representative spent battery-derived adsorbents for pollutant removal.

Adsorbent	Source	Target Pollutant	Adsorbent Dosage	Adsorption Capacity	Ref.
Graphene aerogel	Spent graphite from Spent LIBs	Pb^{2+}	50 mg/L	152.7 mg/g	[159]
Urea-assisted pyrolytic carbon	Waste zinc-carbon batteries	MB	-	330.77 mg/g	[160]
Hydroxyl-functionalized graphene	Waste zinc-carbon batteries	Amoxicillin	1 g/L	36 mg/g	[161]
Graphite oxide	Spent graphite	MG	-	616.99 mg/g	[131]
GO	Spent graphite	Ni^{2+}	-	93.19 mg/g	[131]
AMO@GO	Spent graphite from Spent LIBs	Pb^{2+}	-	353.13 mg/g	[121]
γ-MnO_2	Recycled $LiMn_2O_4$	Co^{2+}	-	0.44 meq/g	[162]
AG@MnO_2	Modified graphite from spent LIBs	Cd^{2+}	0.1 g/L	135.81 mg/g	[163]
MnO_2–AG	Modified graphite from spent LIBs	Pb^{2+}, Cd^{2+}, Ag^{+}	0.2 g/L	-	[164]
SLFP	Spent LIBs	Cu^{2+}, Pb^{2+}, Cd^{2+}, Zn^{2+}	-	44.28, 39.54, 25.63, 27.34 mg/g	[165]
SLMO	Spent LIBs	Cu^{2+}, Pb^{2+}, Cd^{2+}, Zn^{2+}	-	32.51, 31.83, 26.24, 25.25 mg/g	[165]
AlFePO–Li	Spent $LiFePO_4$ batteries	Pb^{2+}	-	723.8 mg/g	[31]
Mm@SiO_2	Spent $LiFePO_4$ batteries	Cu^{2+}, Cd^{2+} Mn^{2+}	-	71.23, 80.31, 68.73 mg/g	[166]
Al-based adsorbent	Spent LIBs	Li^{+}	-	7.44 mg/g	[167]

Graphitic oxide-based materials, including graphite oxide and GO [131], and hydroxyl-functionalized graphene [161], are also derived from waste graphite. These materials feature multilayered lamellar structures and abundant surface oxygen-containing functional groups, which provide active sites for electrostatic attraction and surface complexation. As a result, they are effective in capturing heavy metals, antibiotics, and other organic pollutants from aqueous environments. For instance, graphite oxide exhibits an exceptional adsorption capacity of over 600 mg/g for malachite green (MG) and GO shows excellent adsorption capacity of about 93.19 mg/g for Ni^{2+}.

Metal oxides and mixed materials represent the dominant class of adsorbents derived from spent batteries, particularly those based on manganese dioxide (MnO_2) or its composites with carbon matrices. Amorphous MnO_2-loaded GO (AMO@GO), synthesized from spent $LiMn_2O_4$ [121], and γ-MnO_2 [162] both exhibit high redox activity and ion-exchange capacity, enabling efficient removal of heavy metals such as cobalt, lead, and cadmium. It is worth mentioning that the good adsorption ability of AMO@GO is due to its stable carbon-manganese composite structure with rich oxygen-containing functional groups, whereas that of γ-MnO_2 depends on an ion exchange reaction mechanism. Additionally, MnO_2-modified graphite materials, such as MnO_2-coated amorphous carbon (AG@MnO_2) (Figure 5a) [163] and MnO_2-modified artificial graphite (MnO_2–AG) (Figure 5b) [164], significantly enhance Cd^{2+} adsorption via electrostatic attraction and hydroxyl group–mediated ion exchange. Beyond these composites, direct reuse of cathode powders, such as spent lithium iron phosphate (SLFP) and lithium manganate (SLMO), further supports the "waste-to-treat-waste" strategy [165]. These materials demonstrate chemical adsorption capacities exceeding 40 mg/g for Cu^{2+} and Pb^{2+}, making them cost-effective and environmentally friendly alternatives for heavy metal remediation. Zeolite-type adsorbents are represented by AlFePO–Li, which features a three-dimensional microporous structure and excellent ion-exchange capacity [31]. This material is synthesized from waste $LiFePO_4$ and demonstrates an outstanding adsorption capacity for Pb^{2+}, reaching as high as 723.8 mg/g. The superior performance is attributed to the interaction between protonated amine groups and suspended phosphate sites within the zeolite framework. Magnetic and core–shell composite materials, such as tetraethyl orthosilicate (TEOS) coated Mm (Mm@SiO_2), combine functional surface chemistry with magnetic separability, offering practical advantages for reuse and regeneration [166]. These materials have shown strong removal performance for heavy metals like Cd^{2+} and Cu^{2+}, with adsorption capacities around 80 mg/g. Finally, aluminium-based selective adsorbents, synthesized via co-precipitation of Li^{+} and Al^{3+} from spent battery electrolytes, demonstrate high selectivity toward lithium ions even in the presence of competing cations such as Mg^{2+} and Na^{+} [167]. These materials also exhibit excellent recyclability, retaining over 96% of their original adsorption capacity after multiple adsorption–desorption cycles.

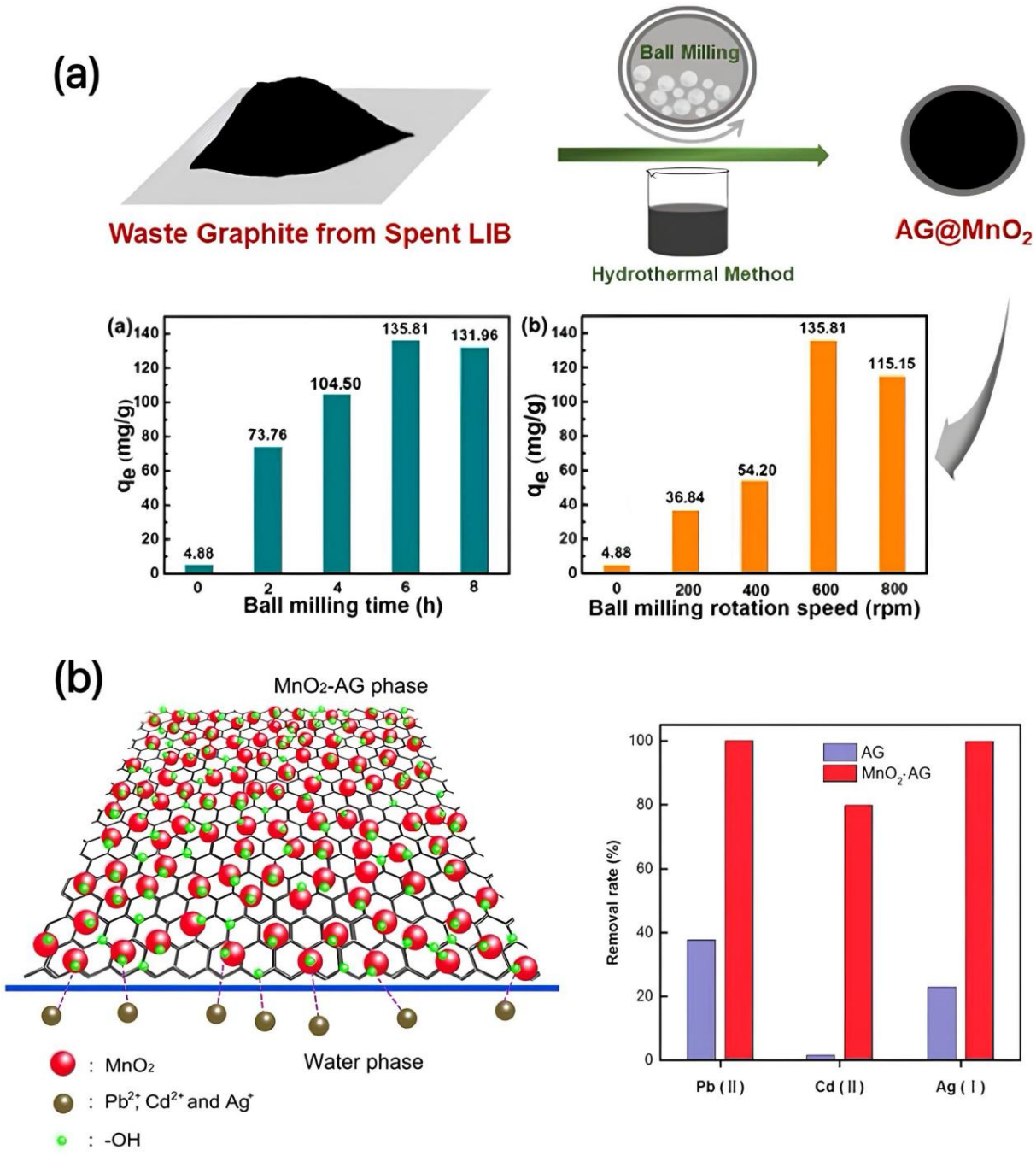

Figure 5. Spent batteries-derived MnO_2-modified graphite materials for pollutant adsorption (**a**) Synthesis process of AG@MnO_2 and the effect of ball milling time and rotation speed on its adsorption capacity [163]. (**b**) Construction of MnO_2–AG and comparison of Pb(II), Cd(II), and Ag(I) removal efficiencies between AG and MnO_2–AG [164].

4. Conclusions and Perspective

In conclusion, spent batteries, once considered hazardous waste, are now recognized as valuable resources for manufacturing high-performance functional materials. Various battery components (including electrode materials, electrolytes, and current collectors) have been successfully converted into catalysts and adsorbents that demonstrate significant effectiveness in wastewater treatment. Looking to the future, several research aspects remain important. Firstly, more systematic methodologies are required to clarify the relationship between the structure of spent battery-derived materials and their catalytic activity, particularly focusing on the roles of defects, dopants, and heterojunctions in enhancing pollutant degradation. Secondly, scalable, low-energy-consumption, and environmentally friendly synthesis methods should be prioritized to ensure practical feasibility. Finally, real-world applications under complex water matrices and long-term stability assessments are essential to bridge the

gap between laboratory-scale experiments and field-scale deployments. Overall, waste battery-derived functional materials hold great promise to drive the advancement of sustainable wastewater treatment technologies.

Author Contributions

Z.X. contributed to the conceptualization, investigation, data curation, and drafting of the original manuscript. Z.C. and B.-J.N. supervised the study, provided project administration and funding acquisition, and contributed to reviewing and editing. X.L. assisted with resources, data curation, and investigation. Z.W. and X.-Y.L. contributed to reviewing and editing parts of the manuscript, participated in discussions, and provided constructive comments. All authors have read and agreed to the published version of the manuscript.

Funding

This work is supported by the Australian Research Council (ARC) Discovery Project (DP220101139) and Linkage Project (LP240100542).

Data Availability Statement

The data supporting the findings of this study are available from the corresponding author upon reasonable request. All data will be preserved for at least 10 years after publication and can be accessed by qualified researchers, provided that privacy and proprietary rights are not violated.

Conflicts of Interest

Given the role as Editor-in-Chief, Bing-Jie Ni had no involvement in the peer review of this paper and had no access to information regarding its peer-review process. Full responsibility for the editorial process of this paper was delegated to another editor of the journal.

References

1. Njema, G.G.; Ouma, R.B.O.; Kibet, J.K. A review on the recent advances in battery development and energy storage technologies. *J. Renew. Energy* **2024**, *2024*, 2329261.
2. Gopi, C.V.M.; Alzahmi, S.; Narayanaswamy, V.; et al. Supercapacitors: A promising solution for sustainable energy storage and diverse applications. *J. Energy Storage* **2025**, *114*, 115729.
3. Zhang, J.; Chen, Z.; Liu, Y.; et al. Removal of emerging contaminants (ECs) from aqueous solutions by modified biochar: A review. *Chem. Eng. J.* **2024**, *479*, 147615.
4. Chen, Z. Clean Technology for Resource, Energy and Environment: Driving Innovation for a Resilient Future. *Clean Technol. Resour. Energy Environ.* **2025**, *1*, 1–4.
5. Wu, J.; Xiao, L.; Shen, L.; et al. Recent advancements in hydrometallurgical recycling technologies of spent lithium-ion battery cathode materials. *Rare Met.* **2024**, *43*, 879–899.
6. Elgarahy, A.M.; Eloffy, M.; Priya, A.; et al. Revitalizing the circular economy: An exploration of e-waste recycling approaches in a technological epoch. *Sustain. Chem. Environ.* **2024**, *7*, 100124.
7. Amusa, H.K.; Sadiq, M.; Alam, G.; et al. Electric vehicle batteries waste management and recycling challenges: A comprehensive review of green technologies and future prospects. *J. Mater. Cycles Waste Manag.* **2024**, *26*, 1959–1978.
8. Chen, Z.; Fang, J.; Wei, W.; et al. Emerging adsorbents for micro/nanoplastics removal from contaminated water: Advances and perspectives. *J. Clean. Prod.* **2022**, *371*, 133676.
9. Chen, Z.; Wei, W.; Ni, B.-J. Prioritizing capture and utilization for microplastic management in water systems. *Nat. Rev. Clean Technol.* **2025**, *1*, 525–527.
10. Zhang, X.; Zhu, M. Recycling spent lithium-ion battery cathode: An overview. *Green Chem.* **2024**, *26*, 7656–7717.
11. Ferdous, A.R.; Shah, S.S.; Shah, S.N.A.; et al. Transforming waste into wealth: Advanced carbon-based electrodes derived from refinery and coal by-products for next-generation energy storage. *Molecules* **2024**, *29*, 2081.
12. Chen, Z.; Zheng, R.; Zou, W.; et al. Integrating high-efficiency oxygen evolution catalysts featuring accelerated surface reconstruction from waste printed circuit boards via a boriding recycling strategy. *Appl. Catal. B: Environ.* **2021**, *298*, 120583.
13. Guo, F.; Chen, Q.; Liu, Z.; et al. Repurposing mining and metallurgical waste as electroactive materials for advanced energy applications: Advances and perspectives. *Catalysts* **2023**, *13*, 1241.
14. Zheng, H.; Chen, Q.; Chen, Z. Carbon-based adsorbents for micro/nano-plastics removal: Current advances and perspectives. *Water Emerg. Contam. Nanoplastics* **2024**, *3*, 11.
15. Li, Y.-Y.; Deng, L.-J.; Cao, Y.-J.; et al. A critical review on the direct regeneration technologies of cathode materials from spent lithium iron phosphate batteries: Y.-Y. Li et al. *Rare Met.* **2025**. https://doi.org/10.1007/s12598-025-03547-w.

16. Gong, H.-Q.; Wang, X.-Y.; Ye, L.; et al. Recycling of spent lithium-ion batteries to resynthesize high-performance cathode materials for sodium-ion storage. *Tungsten* **2024**, *6*, 574–584.
17. Meng, W. Recycling technologies of spent lithium-ion batteries and future directions: A review. *Trans. Nonferrous Met. Soc. China* **2025**, *35*, 271–295.
18. Yang, J.; Zhou, Y.; Zhang, Z.; et al. Effect of electric field on leaching valuable metals from spent lithium-ion batteries. *Trans. Nonferrous Met. Soc. China* **2023**, *33*, 641.
19. Ishmael, A.; Nasser, M.; Abdel-Nasser, M.; et al. Eco-friendly and cost-effective recycling of batteries for utilizing transition metals as catalytic materials for purifying tannery wastewater through Advanced Oxidation Techniques: A critical review. *Nanotechnol. Appl. Sci. J.* **2025**, *1*, 1–28.
20. Wen, G.; Yuan, S.; Dong, Z.; et al. Recycling of spent lithium iron phosphate battery cathode materials: A review. *J. Clean. Prod.* **2024**, *474*, 143625. https://doi.org/10.1016/j.jclepro.2024.143625.
21. Chen, Y.; Zhang, H.; Xiong, Z.; et al. Lithium cobalt oxide with excellent electron mobility: An efficient activator of peroxymonosulfate for the degradation of sulfamethoxazole. *Chem. Eng. J.* **2022**, *445*, 136702.
22. Huang, M.; Wang, M.; Yang, L.; et al. Direct regeneration of spent lithium-ion battery cathodes: From theoretical study to production practice. *Nano-Micro Lett.* **2024**, *16*, 207.
23. Anh Nguyen, T.-H.; Oh, S.-Y. Anode carbonaceous material recovered from spent lithium-ion batteries in electric vehicles for environmental application. *Waste Manag.* **2021**, *120*, 755–761. https://doi.org/10.1016/j.wasman.2020.10.044.
24. Stefan, M.; Kocabas, B.; Güngör, A.; et al. Manganese-doped Zinc Oxide recycled from spent alkaline batteries for photocatalysis and supercapacitor applications. *J. Energy Storage* **2024**, *99*, 113419. https://doi.org/10.1016/j.est.2024.113419.
25. Wink, K.; Hartmann, I. Recent progress in turning waste into catalysts for green syntheses. *Sustain. Chem.* **2024**, *5*, 27–39.
26. Moreira, T.F.M.; Santana, I.L.; Moura, M.N.; et al. Recycling of negative electrodes from spent Ni-Cd batteries as CdO with nanoparticle sizes and its application in remediation of azo dye. *Mater. Chem. Phys.* **2017**, *195*, 19–27. https://doi.org/10.1016/j.matchemphys.2017.04.009.
27. Huang, H.; Liang, W.; Li, R.; et al. Converting spent battery anode waste into a porous biocomposite with high Pb(II) ion capture capacity from solution. *J. Clean. Prod.* **2018**, *184*, 622–631. https://doi.org/10.1016/j.jclepro.2018.03.017.
28. Tan, W.; Ren, W.; Wang, C.; et al. Peroxymonosulfate activated with waste battery-based Mn-Fe oxides for pollutant removal: Electron transfer mechanism, selective oxidation and LFER analysis. *Chem. Eng. J.* **2020**, *394*, 124864. https://doi.org/10.1016/j.cej.2020.124864.
29. Lin, H.; Li, S.; Deng, B.; et al. Degradation of bisphenol A by activating peroxymonosulfate with $Mn_{0.6}Zn_{0.4}Fe_2O_4$ fabricated from spent Zn-Mn alkaline batteries. *Chem. Eng. J.* **2019**, *364*, 541–551. https://doi.org/10.1016/j.cej.2019.01.189.
30. Tang, H.; Li, R.; Fan, X.; et al. A novel S-scheme heterojunction in spent battery-derived $ZnFe_2O_4$/g-C_3N_4 photocatalyst for enhancing peroxymonosulfate activation and visible light degradation of organic pollutant. *J. Environ. Chem. Eng.* **2022**, *10*, 107797. https://doi.org/10.1016/j.jece.2022.107797.
31. Zou, W.; Feng, X.; Wei, W.; et al. Converting spent $LiFePO_4$ battery into zeolitic phosphate for highly efficient heavy metal adsorption. *Inorg. Chem.* **2021**, *60*, 9496–9503.
32. Moretti, A.C.L.; dos Santos, M.G.G.; Soares, M.E.; et al. Degradation of municipal solid waste landfill leachate using ferrites from spent batteries as heterogeneous solar photo-Fenton catalyst. *Int. J. Environ. Res.* **2023**, *17*, 33.
33. Jabbar, W.A.; Jabbar, M.F.A. Modification Graphite of Waste Batteries by Phosphotungstic Acid and Using as Photocatalyst for Methylene Blue Degradation. *Ecol. Eng. Environ. Technol.* **2024**, *25*, 297–307.
34. Fan, M.; Zhang, K.; Gu, X.; et al. Single-Layer Mos_2 Engineered with Recycled Cobalt for Enhanced Activation of Peroxymonosulfate. *Chem. Eng. J.* **2025**, *521*, 166654.
35. Chen, Z.; Zou, W.; Zheng, R.; et al. Synergistic recycling and conversion of spent Li-ion battery leachate into highly efficient oxygen evolution catalysts. *Green Chem.* **2021**, *23*, 6538–6547.
36. Pražanová, A.; Knap, V.; Stroe, D.-I. Literature review, recycling of lithium-ion batteries from electric vehicles, part II: Environmental and economic perspective. *Energies* **2022**, *15*, 7356.
37. Chen, Z.; Wei, W.; Chen, H.; et al. Recent advances in waste-derived functional materials for wastewater remediation. *Eco-Environ. Health* **2022**, *1*, 86–104. https://doi.org/10.1016/j.eehl.2022.05.001.
38. Yu, H.; Yang, H.; Chen, K.; et al. Non–closed–loop recycling strategies for spent lithium–ion batteries: Current status and future prospects. *Energy Storage Mater.* **2024**, *67*, 103288. https://doi.org/10.1016/j.ensm.2024.103288.
39. Chen, Z.; Yun, S.; Wu, L.; et al. Waste-derived catalysts for water electrolysis: Circular economy-driven sustainable green hydrogen energy. *Nano-Micro Lett.* **2023**, *15*, 4.
40. Chen, Z.; Wei, W.; Ni, B.-J.; et al. Plastic wastes derived carbon materials for green energy and sustainable environmental applications. *Environ. Funct. Mater.* **2022**, *1*, 34–48.
41. Chen, Z.; Zheng, R.; Wei, W.; et al. Recycling spent water treatment adsorbents for efficient electrocatalytic water oxidation reaction. *Resour. Conserv. Recycl.* **2022**, *178*, 106037.

42. Wu, X.; Ji, G.; Wang, J.; et al. Toward Sustainable All Solid-State Li–Metal Batteries: Perspectives on Battery Technology and Recycling Processes. *Adv. Mater.* **2023**, *35*, 2301540.
43. Gao, T.; Dai, T.; Fan, N.; et al. Comprehensive review and comparison on pretreatment of spent lithium-ion battery. *J. Environ. Manag.* **2024**, *363*, 121314.
44. Jin, S.; Mu, D.; Lu, Z.; et al. A comprehensive review on the recycling of spent lithium-ion batteries: Urgent status and technology advances. *J. Clean. Prod.* **2022**, *340*, 130535.
45. Xu, Z.; Zhiyuan, L.; Wenjun, M.; et al. Pretreatment options for the recycling of spent lithium-ion batteries: A comprehensive review. *J. Energy Storage* **2023**, *72*, 108691.
46. Wu, X.; Ma, J.; Wang, J.; et al. Progress, key issues, and future prospects for li-ion battery recycling. *Glob. Chall.* **2022**, *6*, 2200067.
47. Li, Y.; Lv, W.; Huang, H.; et al. Recycling of spent lithium-ion batteries in view of green chemistry. *Green Chem.* **2021**, *23*, 6139–6171.
48. Kaya, M.; Delavandani, H. State-of-the-Art Lithium-Ion Battery Pretreatment Methods for the Recovery of Critical Metals. *Minerals* **2025**, *15*, 546.
49. Khodadadmahmoudi, G.; Javdan Tabar, K.; Homayouni, A.H.; et al. Recycling spent lithium batteries–an overview of pretreatment flowsheet development based on metallurgical factors. *Environ. Technol. Rev.* **2023**, *12*, 2248559.
50. Fang, Z.; Duan, Q.; Peng, Q.; et al. Comparative study of chemical discharge strategy to pretreat spent lithium-ion batteries for safe, efficient, and environmentally friendly recycling. *J. Clean. Prod.* **2022**, *359*, 132116.
51. Zhang, H.; Zhao, H.; Khan, M.A.; et al. Recent progress in advanced electrode materials, separators and electrolytes for lithium batteries. *J. Mater. Chem. A* **2018**, *6*, 20564–20620.
52. Kim, S.; Bang, J.; Yoo, J.; et al. A comprehensive review on the pretreatment process in lithium-ion battery recycling. *J. Clean. Prod.* **2021**, *294*, 126329.
53. Xiao, J.; Guo, J.; Zhan, L.; et al. A cleaner approach to the discharge process of spent lithium ion batteries in different solutions. *J. Clean. Prod.* **2020**, *255*, 120064.
54. Rouhi, H.; Karola, E.; Serna-Guerrero, R.; et al. Voltage behavior in lithium-ion batteries after electrochemical discharge and its implications on the safety of recycling processes. *J. Energy Storage* **2021**, *35*, 102323.
55. Nembhard, N. Safe, Sustainable Discharge of Electric Vehicle Batteries as a Pre-Treatment Step to Crushing in the Recycling Process. Master's Thesis, Universitat Politècnica de Catalunya, Barcelona, Spain, 2020.
56. Wang, H.; Qu, G.; Yang, J.; et al. An effective and cleaner discharge method of spent lithium batteries. *J. Energy Storage* **2022**, *54*, 105383.
57. Ali, H.; Khan, H.A.; Pecht, M. Preprocessing of spent lithium-ion batteries for recycling: Need, methods, and trends. *Renew. Sustain. Energy Rev.* **2022**, *168*, 112809.
58. Harper, G.; Sommerville, R.; Kendrick, E.; et al. Recycling lithium-ion batteries from electric vehicles. *Nature* **2019**, *575*, 75–86.
59. Ali, H.; Khan, H.A.; Pecht, M.G. Circular economy of Li Batteries: Technologies and trends. *J. Energy Storage* **2021**, *40*, 102690.
60. Ji, Y.; Kpodzro, E.E.; Jafvert, C.T.; et al. Direct recycling technologies of cathode in spent lithium-ion batteries. *Clean Technol. Recycl.* **2021**, *1*, 124–151.
61. Glöser-Chahoud, S.; Huster, S.; Rosenberg, S.; et al. Industrial disassembling as a key enabler of circular economy solutions for obsolete electric vehicle battery systems. *Resour. Conserv. Recycl.* **2021**, *174*, 105735.
62. Shi, M.; Ren, Y.; Cao, J.; et al. Current Situation and Development Prospects of Discharge Pretreatment during Recycling of Lithium-ion Batteries: A Review. *Batter. Supercaps* **2024**, *7*, e202300477.
63. Ye, L.; Wang, C.; Cao, L.; et al. Effective regeneration of high-performance anode material recycled from the whole electrodes in spent lithium-ion batteries via a simplified approach. *Green Energy Environ.* **2021**, *6*, 725–733.
64. Piątek, J.; Afyon, S.; Budnyak, T.M.; et al. Sustainable Li-ion batteries: Chemistry and recycling. *Adv. Energy Mater.* **2021**, *11*, 2003456.
65. Lei, C.; Aldous, I.; Hartley, J.M.; et al. Lithium ion battery recycling using high-intensity ultrasonication. *Green Chem.* **2021**, *23*, 4710–4715.
66. Thompson, D.; Hyde, C.; Hartley, J.M.; et al. To shred or not to shred: A comparative techno-economic assessment of lithium ion battery hydrometallurgical recycling retaining value and improving circularity in LIB supply chains. *Resour. Conserv. Recycl.* **2021**, *175*, 105741.
67. Liu, C.; Qiu, X.; Liu, Y.; et al. Research status and prospects of physical separation technology of spent lithium-ion batteries. *Chin J Rare Met* **2021**, *45*, 493.
68. Zhang, Y.; Zhao, M. Cloud-based in-situ battery life prediction and classification using machine learning. *Energy Storage Mater.* **2023**, *57*, 346–359.

69. Dolotko, O.; Hlova, I.Z.; Mudryk, Y.; et al. Mechanochemical recovery of Co and Li from LCO cathode of lithium-ion battery. *J. Alloys Compd.* **2020**, *824*, 153876.
70. Al-Shammari, H.; Farhad, S. Heavy liquids for rapid separation of cathode and anode active materials from recycled lithium-ion batteries. *Resour. Conserv. Recycl.* **2021**, *174*, 105749.
71. Verdugo, L.; Zhang, L.; Saito, K.; et al. Flotation behavior of the most common electrode materials in lithium ion batteries. *Sep. Purif. Technol.* **2022**, *301*, 121885.
72. Zhu, X.; Zhang, C.; Feng, P.; et al. A novel pulsated pneumatic separation with variable-diameter structure and its application in the recycling spent lithium-ion batteries. *Waste Manag.* **2021**, *131*, 20–30.
73. Cao, Y.; Wang, Z.; Wang, J.; et al. Multi-stage electrostatic separation for recovering of aluminum from fine granules of black dross. *J. Wuhan Univ. Technol.-Mater. Sci. Ed.* **2019**, *34*, 925–931.
74. Silveira, A.; Santana, M.; Tanabe, E.; et al. Recovery of valuable materials from spent lithium ion batteries using electrostatic separation. *Int. J. Miner. Process.* **2017**, *169*, 91–98.
75. Fan, M.-C.; Zhao, Y.; Kang, Y.-Q.; et al. Room-temperature extraction of individual elements from charged spent LiFePO4 batteries. *Rare Met.* **2022**, *41*, 1595–1604.
76. Zhu, X.; Nie, C.; Wang, S.; et al. Cleaner approach to the recycling of metals in waste printed circuit boards by magnetic and gravity separation. *J. Clean. Prod.* **2020**, *248*, 119235.
77. Zhu, X.; Nie, C.; Zhang, H.; et al. Recovery of metals in waste printed circuit boards by flotation technology with soap collector prepared by waste oil through saponification. *Waste Manag.* **2019**, *89*, 21–26.
78. Vanderbruggen, A.; Salces, A.; Ferreira, A.; et al. Improving separation efficiency in end-of-life lithium-ion batteries flotation using attrition pre-treatment. *Minerals* **2022**, *12*, 72.
79. Zhang, G.; Yuan, X.; He, Y.; et al. Recent advances in pretreating technology for recycling valuable metals from spent lithium-ion batteries. *J. Hazard. Mater.* **2021**, *406*, 124332.
80. Bi, H.; Zhu, H.; Zu, L.; et al. A new model of trajectory in eddy current separation for recovering spent lithium iron phosphate batteries. *Waste Manag.* **2019**, *100*, 1–9.
81. Huang, Z.; Zhu, J.; Wu, X.; et al. Eddy current separation can be used in separation of non-ferrous particles from crushed waste printed circuit boards. *J. Clean. Prod.* **2021**, *312*, 127755.
82. Smith, Y.R.; Nagel, J.R.; Rajamani, R.K. Eddy current separation for recovery of non-ferrous metallic particles: A comprehensive review. *Miner. Eng.* **2019**, *133*, 149–159.
83. Kong, L.; Liu, F.; Hu, X.; et al. An improved pretreatment method for recovering cathode materials from lithium-ion battery: Ultrasonic-assisted NaOH-enhanced dissolving. *Energy Sources Part A Recovery Util. Environ. Eff.* **2023**, *45*, 877–887.
84. Yang, F.; Chen, X.; Qu, G.; et al. Electrode separation via water electrolysis for sustainable battery recycling. *Nat. Sustain.* **2025**, *8*, 520–529.
85. Lv, X.; Deng, F.; Liu, H.; et al. Recycling different crystal forms of MnO2 from spent Li-ion batteries cathodes for SDZ degradation. *J. Environ. Chem. Eng.* **2024**, *12*, 111622. https://doi.org/10.1016/j.jece.2023.111622.
86. Mylarappa, M.; Lakshmi, V.V.; Mahesh, K.V.; et al. A facile hydrothermal recovery of nano sealed MnO_2 particle from waste batteries: An advanced material for electrochemical and environmental applications. *IOP Conf. Ser. Mater. Sci. Eng.* **2016**, *149*, 012178.
87. Zou, W.; Li, J.; Wang, R.; et al. Hydroxylamine mediated Fenton-like interfacial reaction dynamics on sea urchin-like catalyst derived from spent $LiFePO_4$ battery. *J. Hazard. Mater.* **2022**, *431*, 128590. https://doi.org/10.1016/j.jhazmat.2022.128590.
88. Xu, L.; Chen, C.; Huo, J.-B.; et al. Iron hydroxyphosphate composites derived from waste lithium-ion batteries for lead adsorption and Fenton-like catalytic degradation of methylene blue. *Environ. Technol. Innov.* **2019**, *16*, 100504.
89. Niu, Z.; Tao, X.; Huang, H.; et al. Green synthesis of magnetically recyclable $Mn_{0.6}Zn_{0.4}Fe_2O_4$@Zn1-xMnxS composites from spent batteries for visible light photocatalytic degradation of phenol. *Chemosphere* **2022**, *287*, 132238. https://doi.org/10.1016/j.chemosphere.2021.132238.
90. Chen, X.; Deng, F.; Liu, X.; et al. Hydrothermal synthesis of MnO_2/Fe(0) composites from Li-ion battery cathodes for destructing sulfadiazine by photo-Fenton process. *Sci. Total Environ.* **2021**, *774*, 145776. https://doi.org/10.1016/j.scitotenv.2021.145776.
91. Yan, S.; Chen, X.; Yang, Y.; et al. Peroxymonosulfate activation by N-doped 3D graphene from spent lithium-ion batteries for organic pollutants degradation: An insight into the degradation mechanism. *Chem. Eng. J.* **2024**, *484*, 149379. https://doi.org/10.1016/j.cej.2024.149379.
92. Wu, N.; Zhang, X.; Zhang, X.; et al. Simultaneous degradation of trace antibiotics in water by adsorption and catalytic oxidation induced by N-doped reduced graphene oxide (N-rGO): Synergistic mechanism. *Mater. Res. Express* **2022**, *9*, 065601.

93. Kumar, K.Y.; Prashanth, M.K.; Shanavaz, H.; et al. Spent Li-ion batteries derived synthesis of boron doped RGO-Bi2WO6 for photocatalytic degradation of antibiotics. *Appl. Surf. Sci. Adv.* **2024**, *19*, 100569. https://doi.org/10.1016/j.apsadv.2023.100569.
94. Annamalai, K.; Annamalai, A.; Ravichandran, R.; et al. Recyclable waste dry-cell batteries derived carbon dots (CDs) for detection of two-fold metal ions and degradation of BTB dye. *Waste Manag.* **2023**, *163*, 61–72. https://doi.org/10.1016/j.wasman.2023.03.032.
95. Li, R.; Hu, H.; Ma, Y.; et al. Persulfate enhanced photocatalytic degradation of bisphenol A over wasted batteries-derived ZnFe2O4 under visible light. *J. Clean. Prod.* **2020**, *276*, 124246. https://doi.org/10.1016/j.jclepro.2020.124246.
96. Ribeiro, J.; Moreira, T.; Santana, I.; et al. Sol-gel synthesis, characterization, and catalytic properties of Ni, Cd, Co, and Fe oxides recycled from spent Ni-Cd batteries using citric acid as a leaching agent. *Mater. Chem. Phys.* **2018**, *205*, 186–194.
97. Cheng, C.; Chang, L.; Zhang, X.; et al. Interface engineering-induced perovskite/spinel $LaCoO_3/Co_3O_4$ heterostructured nanocomposites for efficient peroxymonosulfate activation to degrade levofloxacin. *Environ. Res.* **2023**, *229*, 115994. https://doi.org/10.1016/j.envres.2023.115994.
98. Ma, Y.; Wang, D.; Xu, Y.; et al. Nonradical electron transfer-based peroxydisulfate activation by a Mn−Fe bimetallic oxide derived from spent alkaline battery for the oxidation of bisphenol A. *J. Hazard. Mater.* **2022**, *436*, 129172. https://doi.org/10.1016/j.jhazmat.2022.129172.
99. Xu, L.; Liang, L.; Chen, C.; et al. Upcycling spent lithium battery cathodes into efficient PMS catalysts for organic contaminants degradation. *J. Environ. Chem. Eng.* **2023**, *11*, 111605. https://doi.org/10.1016/j.jece.2023.111605.
100. Al-Madhagi, H.; Yazbik, V.; Abdelwahed, W.; et al. Magnetite nanoparticle Co-precipitation synthesis, characterization, and applications: Mini review. *Bionanoscience* **2023**, *13*, 853–859.
101. Rocha, A.K.S.; Magnago, L.B.; Santos, J.J.; et al. Copper ferrite synthesis from spent Li-ion batteries for multifunctional application as catalyst in photo Fenton process and as electrochemical pseudocapacitor. *Mater. Res. Bull.* **2019**, *113*, 231–240. https://doi.org/10.1016/j.materresbull.2019.02.007.
102. Moura, M.N.; Barrada, R.V.; Almeida, J.R.; et al. Synthesis, characterization and photocatalytic properties of nanostructured $CoFe_2O_4$ recycled from spent Li-ion batteries. *Chemosphere* **2017**, *182*, 339–347. https://doi.org/10.1016/j.chemosphere.2017.05.036.
103. Betim, F.S.; Marins, A.A.L.; Coelho, E.L.D.; et al. Evaluation of photocatalytic properties of zinc and cobalt mixed oxide recycled from spent Li-ion and Zn–MnO_2 batteries in photo-Fenton-like process. *Mater. Res. Bull.* **2023**, *162*, 112179. https://doi.org/10.1016/j.materresbull.2023.112179.
104. Liang, J.; Xue, Y.; Gu, J.; et al. Sustainably recycling spent lithium-ion batteries to prepare magnetically separable cobalt ferrite for catalytic degradation of bisphenol A via peroxymonosulfate activation. *J. Hazard. Mater.* **2022**, *427*, 127910. https://doi.org/10.1016/j.jhazmat.2021.127910.
105. Zhao, Y.; Wang, H.; Ji, J.; et al. Degradation of ciprofloxacin by peroxymonosulfate activation using catalyst derived from spent lithium-ion batteries. *J. Clean. Prod.* **2022**, *362*, 132442. https://doi.org/10.1016/j.jclepro.2022.132442.
106. Zhao, Y.; Yuan, X.; Jiang, L.; et al. Reutilization of cathode material from spent batteries as a heterogeneous catalyst to remove antibiotics in wastewater via peroxymonosulfate activation. *Chem. Eng. J.* **2020**, *400*, 125903. https://doi.org/10.1016/j.cej.2020.125903.
107. Gao, M.; Wei, H.; Teng, R.; et al. One-step calcination of Ni/Co/Mn ternary catalysts from spent lithium-ion batteries for iopamidol degradation via peroxymonosulfate activation. *J. Water Process Eng.* **2024**, *59*, 104996. https://doi.org/10.1016/j.jwpe.2024.104996.
108. Xu, Y.; Ai, J.; Zhang, H. The mechanism of degradation of bisphenol A using the magnetically separable $CuFe_2O_4$/peroxymonosulfate heterogeneous oxidation process. *J. Hazard. Mater.* **2016**, *309*, 87–96. https://doi.org/10.1016/j.jhazmat.2016.01.023.
109. Chen, H.; Wei, Y.; Han, C.; et al. Peroxymonosulfate activation by CoO@C catalyst from integrated recycling of spent lithium-ion battery: Performance and mechanism. *Sep. Purif. Technol.* **2025**, *355*, 129658. https://doi.org/10.1016/j.seppur.2024.129658.
110. Zhou, D.; Tang, R.; Min, Y.; et al. External electric field-assisted electronic restructuring of transition metal oxides derived from spent lithium-ion batteries to enhance persulfate activation. *Appl. Surf. Sci.* **2023**, *625*, 157120. https://doi.org/10.1016/j.apsusc.2023.157120.
111. Deng, B.; Wang, Z.; Chen, W.; et al. Phase controlled synthesis of transition metal carbide nanocrystals by ultrafast flash Joule heating. *Nat. Commun.* **2022**, *13*, 262. https://doi.org/10.1038/s41467-021-27878-1.
112. Dong, Q.; Yao, Y.; Cheng, S.; et al. Programmable heating and quenching for efficient thermochemical synthesis. *Nature* **2022**, *605*, 470–476. https://doi.org/10.1038/s41586-022-04568-6.
113. Yu, F.; Jia, C.; Wu, X.; et al. Rapid self-heating synthesis of Fe-based nanomaterial catalyst for advanced oxidation. *Nat. Commun.* **2023**, *14*, 4975. https://doi.org/10.1038/s41467-023-40691-2.
114. Shang, H.; Yang, W.; He, Z.; et al. Flash Joule Heating Upgraded Li Leaching of Residues from Spent LiFePO4 Cathodes for Superior Catalytic Degradation of Pollutants. *ACS ES&T Eng.* **2025**, *5*, 724–731.

115. Yan, X.; Wang, B.; Ji, M.; et al. In-Situ Synthesis of CQDs/BiOBr Material via Mechanical Ball Milling with Enhanced Photocatalytic Performances. *Chin. J. Struct. Chem.* **2022**, *41*, 2208044–2208051. https://doi.org/10.14102/j.cnki.0254-5861.2022-0141.
116. Joy, J.; Krishnamoorthy, A.; Tanna, A.; et al. Recent developments on the synthesis of nanocomposite materials via ball milling approach for energy storage applications. *Appl. Sci.* **2022**, *12*, 9312.
117. Qin, H.; Liu, Y.; Liu, H.; et al. Application and Research Progress of Nanomaterials as Adsorbents in Environment Field. In *Carbon Nanomaterials and their Composites as Adsorbents*; Springer: Cham, Switzerland, 2024; pp. 105-134.
118. Chen, Z.; Han, G.-F.; Mahmood, A.; et al. Mechanosynthesized electroactive materials for sustainable energy and environmental applications: A critical review. *Prog. Mater. Sci.* **2024**, *145*, 101299.
119. Wei, L.K.; Abd Rahim, S.Z.; Al Bakri Abdullah, M.M.; et al. Producing metal powder from machining chips using ball milling process: A review. *Materials* **2023**, *16*, 4635.
120. Zhang, L.; Huang, S.; Ding, Y.; et al. Research progress in the preparation of sodium-ion battery anode materials using ball milling. *RSC Adv.* **2025**, *15*, 6324–6341.
121. Yan, R.; Li, B.; Zhou, M.; et al. Highly-efficient synthesis of heavy metal adsorbents by using spent lithium-ion battery anode graphite via one-step mechanochemistry process. *Resour. Conserv. Recycl.* **2023**, *190*, 106857. https://doi.org/10.1016/j.resconrec.2022.106857.
122. Arriola-Villaseñor, E.; Ardila Arias, A.N.; Bedoya Betancour, S.; et al. Graphene Recovery in Both Dispersed and Decanted Fractions from Lithium-Ion Battery Graphite via Sonication. *Recycling* **2025**, *10*, 119.
123. Fernández-Martínez, R.; Ortiz, I.; Gómez-Mancebo, M.B.; et al. Transformation of Graphite Recovered from Batteries into Functionalized Graphene-Based Sorbents and Application to Gas Desulfurization. *Molecules* **2024**, *29*, 3577.
124. Wang, Y.; Yang, Z.; Zhang, C.; et al. Fabricating carbon quantum dots of graphitic carbon nitride vis ultrasonic exfoliation for highly efficient H2O2 production. *Ultrason. Sonochemistry* **2023**, *99*, 106582.
125. Wen, Y.; Liu, H.; Jiang, X. Preparation of graphene by exfoliation and its application in lithium-ion batteries. *J. Alloys Compd.* **2023**, *961*, 170885.
126. Wang, S.; Yu, Y.; Meng, J. A Review of the Sonication-Assisted Exfoliation Methods for MoX2 (X: S, Se, Te) Using Water and Ethanol. *Arch. Acoust.* **2025**, *50*, 137–145.
127. Ayub, M.N.; Shahzad, U.; Saeed, M.; et al. Modern innovations in the provision and efficient application of 2D inorganic nanoscale materials. *Rev. Inorg. Chem.* **2025**, *45*, 175–206.
128. An, C.; Wang, T.; Wang, S.; et al. Ultrasonic-assisted preparation of two-dimensional materials for electrocatalysts. *Ultrason. Sonochemistry* **2023**, *98*, 106503.
129. Budiarso, I.J.; Dabur, V.A.; Rachmantyo, R.; et al. Carbon nitride-and graphene-based materials for the photocatalytic degradation of emerging water pollutants. *Mater. Adv.* **2024**, *5*, 2668.
130. Haris, M.; Usman, M.; Saleem, A.; et al. Synthesis of conch-like layered carbon nanosheets by ball-milling assisted ultrasonic exfoliation for highly selective removal of Cd (II) from multiple water matrices. *Sep. Purif. Technol.* **2023**, *325*, 124756.
131. Premathilake, D.S.; Colombi, F.; Botelho Junior, A.B.; et al. Recycling lithium-ion battery graphite: Synthesis of adsorbent materials for highly efficient removal of dye and metal ions from wastewater. *Results Eng.* **2024**, *22*, 102232. https://doi.org/10.1016/j.rineng.2024.102232.
132. Feng, L.; Liao, X.; Wu, M.; et al. Enhanced removal of ammonia induced by the co-existing halogenated organics in wastewater via reutilization of spent lithium-ion batteries for peroxymonosulfate activation. *Chem. Eng. J.* **2023**, *470*, 144430. https://doi.org/10.1016/j.cej.2023.144430.
133. Chiao, Y.-W.; Liao, W.; Krisbiantoro, P.A.; et al. Waste-battery-derived multifunctional zinc catalysts for glycolysis and decolorization of polyethylene terephthalate. *Appl. Catal. B Environ.* **2023**, *325*, 122302. https://doi.org/10.1016/j.apcatb.2022.122302.
134. Shrestha, A.B.; Amarasekara, A.S. The sustainable and green management of spent lithium-ion batteries through hydroxy acid recycling and direct regeneration of active positive electrode material: A review. *Batteries* **2025**, *11*, 68.
135. Schmitz, D.; Prasetyo, H.; Birich, A.; et al. Co-Precipitation of Metal Oxalates from Organic Leach Solution Derived from Spent Lithium-Ion Batteries (LIBs). *Metals* **2024**, *14*, 80.
136. Quirino, A.G.C.; Viana, G.C.C.; Cahino, A.M.; et al. Catalysts from post-consumer batteries waste for photodegradation of contaminants: a systematic analysis. *Rev. Gestão Soc. E Ambient.* **2025**, *19*, 1–18.
137. Wang, P.; Guo, Y.; Guan, J.; et al. Applications of spent lithium battery electrode materials in catalytic decontamination: A review. *Catalysts* **2023**, *13*, 189.
138. González-Fernández, C.; Bringas, E.; Rivero, M.J.; et al. Revealing the role of magnetic materials in light-driven advanced oxidation processes: Enhanced degradation of contaminants and facilitated magnetic recovery. *Front. Chem. Eng.* **2024**, *6*, 1430773.

139. Gasim, M.F.; Lim, J.-W.; Low, S.-C.; et al. Can biochar and hydrochar be used as sustainable catalyst for persulfate activation? *Chemosphere* **2022**, *287*, 132458.
140. Li, N.; Wu, S.; Dai, H.; et al. Thermal activation of persulfates for organic wastewater purification: Heating modes, mechanism and influencing factors. *Chem. Eng. J.* **2022**, *450*, 137976.
141. Gujar, S.K.; Divyapriya, G.; Gogate, P.R.; et al. Environmental applications of ultrasound activated persulfate/peroxymonosulfate oxidation process in combination with other activating agents. *Crit. Rev. Environ. Sci. Technol.* **2023**, *53*, 780–802.
142. Qian, X.; Ji, J.; Zhao, Y.; et al. Rational design of waste anode graphite-derived carbon catalyst to activate peroxymonosulfate for atrazine degradation. *Environ. Res.* **2024**, *257*, 119296. https://doi.org/10.1016/j.envres.2024.119296.
143. Wang, Z.; Ma, Y.; Lin, H.; et al. Zn-Mn bimetallic oxide derived from waste battery to activate peroxymonosulfate for bisphenol A removal under visible light irradiation. *J. Environ. Chem. Eng.* **2024**, *12*, 113351. https://doi.org/10.1016/j.jece.2024.113351.
144. De-Nasri, S.J.; Nagarajan, S.; Robertson, P.K.; et al. Quantification of hydroxyl radicals in photocatalysis and acoustic cavitation: Utility of coumarin as a chemical probe. *Chem. Eng. J.* **2021**, *420*, 127560.
145. Dai, M.; Niu, Q.; Wu, S.; et al. Hydroxyl radicals in ozone-based advanced oxidation of organic contaminants: A review. *Environ. Chem. Lett.* **2024**, *22*, 3059–3106.
146. Mancipe, S.; Romanelli, G.P.; Martínez, J.J.; et al. Formation of Hydroxyl Radicals in Advanced Oxidation Processes for the Degradation of Contaminated Organic Matter. *Curr. Green Chem.* **2025**, *12*, 117–137.
147. Sun, W.; Dong, H.; Wang, Y.; et al. Ultraviolet (UV)-based advanced oxidation processes for micropollutant abatement in water treatment: Gains and problems. *J. Environ. Chem. Eng.* **2023**, *11*, 110425.
148. Guan, J.; Li, Z.; Chen, S.; et al. Zero-valent iron supported on expanded graphite from spent lithium-ion battery anodes and ferric chloride for the degradation of 4-chlorophenol in water. *Chemosphere* **2022**, *290*, 133381. https://doi.org/10.1016/j.chemosphere.2021.133381.
149. Xu, Z.; Wang, J.; Sun, S.; et al. Simple route for graphite recycling from waste lithium-ion batteries to environmental functional materials. *ACS Sustain. Chem. Eng.* **2022**, *10*, 13435–13443.
150. Bayat, N.; Sheibani, S. Efficient photocatalytic activity of $ZnMn_2O_4$ nanopowder synthesized by mechano-thermal recycling of alkaline and Zn/C spent batteries. *Ceram. Int.* **2024**, *50*, 14757–14772. https://doi.org/10.1016/j.ceramint.2024.01.390.
151. Kékedy-Nagy, L.; English, L.; Anari, Z.; et al. Electrochemical nutrient removal from natural wastewater sources and its impact on water quality. *Water Res.* **2022**, *210*, 118001.
152. Wang, Y.; Lin, Y.; He, S.; et al. Singlet oxygen: Properties, generation, detection, and environmental applications. *J. Hazard. Mater.* **2024**, *461*, 132538.
153. Xie, Z.-H.; He, C.-S.; Pei, D.-N.; et al. Review of characteristics, generation pathways and detection methods of singlet oxygen generated in advanced oxidation processes (AOPs). *Chem. Eng. J.* **2023**, *468*, 143778. https://doi.org/10.1016/j.cej.2023.143778.
154. Barrios, B.; Mohrhardt, B.; Doskey, P.V.; et al. Mechanistic insight into the reactivities of aqueous-phase singlet oxygen with organic compounds. *Environ. Sci. Technol.* **2021**, *55*, 8054–8067.
155. Wen, Y.; Zhou, J.; He, L.; et al. Oxygen-deficient $MnCO_3$ based on waste alkaline Zn-MnO_2 battery as an enhanced activator for peroxymonosulfate removing Oxytetracycline hydrochloride. *J. Water Process Eng.* **2024**, *68*, 106307. https://doi.org/10.1016/j.jwpe.2024.106307.
156. Zhao, Y.; Wang, H.; Ji, J.; et al. Recycling of waste power lithium-ion batteries to prepare nickel/cobalt/manganese-containing catalysts with inter-valence cobalt/manganese synergistic effect for peroxymonosulfate activation. *J. Colloid Interface Sci.* **2022**, *626*, 564–580. https://doi.org/10.1016/j.jcis.2022.06.112.
157. Li, B.; Ma, B.; Wei, M.; et al. Synthesis of Co-NC catalysts from spent lithium-ion batteries for fenton-like reaction: Generation of singlet oxygen with ~100% selectivity. *Carbon* **2022**, *197*, 76–86. https://doi.org/10.1016/j.carbon.2022.06.029.
158. Kosenko, A.; Pushnitsa, K.; Pavlovskii, A.A.; et al. The Review of Existing Strategies of End-of-Life Graphite Anode Processing Using 3Rs Approach: Recovery, Recycle, Reuse. *Batteries* **2023**, *9*, 579.
159. Zheng, Y.; Liu, X.; Liu, S.; et al. Constructing physical and chemical synergistic effect of graphene aerogels regenerated from spent graphite anode of lithium ion batteries achieves high efficient adsorption of lead in wastewater. *Appl. Surf. Sci.* **2023**, *633*, 157623. https://doi.org/10.1016/j.apsusc.2023.157623.
160. Pang, W.; Zhai, M.; Li, C.; et al. Upcycling of Battery Separator Waste into High-Value Carbon Materials for Efficient Industrial Pollutant Adsorption. *ACS Sustain. Chem. Eng.* **2025**, *13*, 9510–9521.
161. Aguilar, J.C.S.; Lawagon, C.P.; Gallawan, J.M.M.; et al. Hydroxyl-functionalized Graphene from Spent Batteries as Efficient Adsorbent for Amoxicillin. *CET J.-Chem. Eng. Trans.* **2021**, *86*, 331—336
162. Zhang, Y.; Li, X.; Chen, X.; et al. Tunnel manganese oxides prepared using recovered $LiMn_2O_4$ from spent lithium-ion batteries: Co adsorption behavior and mechanism. *J. Hazard. Mater.* **2022**, *425*, 127957. https://doi.org/10.1016/j.jhazmat.2021.127957.
163. Hao, J.; Meng, X.; Fang, S.; et al. MnO_2-functionalized amorphous carbon sorbents from spent lithium-ion batteries for highly efficient removal of cadmium from aqueous solutions. *Ind. Eng. Chem. Res.* **2020**, *59*, 10210–10220.
164. Zhao, T.; Yao, Y.; Wang, M.; et al. Preparation of MnO_2-modified graphite sorbents from spent Li-ion batteries for the treatment of water contaminated by lead, cadmium, and silver. *ACS Appl. Mater. Interfaces* **2017**, *9*, 25369–25376.

165. Zhang, Y.; Wang, Y.; Zhang, H.; et al. Recycling spent lithium-ion battery as adsorbents to remove aqueous heavy metals: Adsorption kinetics, isotherms, and regeneration assessment. *Resour. Conserv. Recycl.* **2020**, *156*, 104688. https://doi.org/10.1016/j.resconrec.2020.104688.
166. Zou, W.; Feng, X.; Wang, R.; et al. High-efficiency core-shell magnetic heavy-metal absorbents derived from spent-$LiFePO_4$ Battery. *J. Hazard. Mater.* **2021**, *402*, 123583. https://doi.org/10.1016/j.jhazmat.2020.123583.
167. Wu, J.; Liu, B.; Qian, J.; et al. Facile synthesis of aluminum-based adsorbents from spent lithium-ion batteries for efficient Li+ extraction. *J. Environ. Chem. Eng.* **2025**, *13*, 117000. https://doi.org/10.1016/j.jece.2025.117000.